

OPEN

Accelerated degradation of cFLIP_L and sensitization of the TRAIL DISC-mediated apoptotic cascade by pinoresinol, a lignan isolated from *Rubia philippinensis*

So-Ra Lee¹, Khong Trong Quan², Hee Sun Byun¹, InWha Park², Kidong Kang¹, Xuezhe Piao¹, Eunjin Ju¹, Hyunju Ro³, MinKyun Na² & Gang Min Hur¹

Plant-derived lignans have numerous biological effects including anti-tumor and anti-inflammatory activities. Screening of purified constituents of *Rubia philippinensis* from human glioblastoma cells resistant to TNF-related apoptosis-inducing ligand (TRAIL) has suggested that the lignan pinoresinol was a highly active TRAIL sensitizer. Here we show that treatment with nontoxic doses of pinoresinol in combination with TRAIL induced rapid apoptosis and caspase activation in many types of glioblastoma cells, but not in normal astrocytes. Analyses of apoptotic signaling events revealed that pinoresinol enhanced the formation of TRAIL-mediated death-inducing signaling complex (DISC) and complete processing of procaspase-8 within the DISC in glioblastoma cells, in which caspase-8 was inactivated. Mechanistically, pinoresinol downregulated the expression of cellular FLICE-inhibitory protein (cFLIP_L) and survivin through proteasome-mediated degradation, without affecting death receptors or downstream intracellular apoptosis-related proteins. Furthermore, the sensitization of TRAIL-mediated apoptosis by pinoresinol strictly depended on the expression level of cFLIP_L, which was regulated through *de novo* protein synthesis, rather than by NF-κB or p53 signaling. Taken together, our results indicate that pinoresinol facilitates DISC-mediated caspase-8 activation by targeting cFLIP_L in an early event in apoptotic signaling, which provides a potential therapeutic module for TRAIL-based chemotherapy.

The use of TNF-related apoptosis-inducing ligand (TRAIL) in cancer therapy has long been thought as an attractive strategy because it can selectively target cancer cells without affecting the majority of normal human cells¹. The anti-cancer activity of TRAIL is attributable to its ability to elicit apoptosis through binding of its functional receptors, death receptors 4 and 5 (DR4 and DR5), and subsequent association with an adaptor protein, Fas-associated death domain (FADD)². During apoptosis, FADD recruits the initiator caspases (procaspase-8 and/or procaspase-10) for the assembly of a death-inducing signaling complex (DISC). Within the DISC, the oligomerization and cleavage of the initiator caspases are the critical upstream events for activation of either the executioner caspase-3 cascade or mitochondrial-dependent apoptotic pathway via Bid cleavage, leading to sufficient apoptosis upon TRAIL treatment, depending on the specific cell type^{3,4}. Importantly, genetic lesions in the components of TRAIL signaling have been found in human malignant cancers, suggesting that TRAIL functions in immune surveillance against developing cancers and metastasis⁵⁻⁷. Indeed, mice null of TRAIL receptor were shown to be susceptible to inflammation and tumorigenesis with apoptotic defects⁸. Consistent with this possibility, currently evaluated TRAIL agonistic antibodies have demonstrated a significant therapeutic efficacy in a number of preclinical studies^{9,10}. However, therapeutic benefits in clinical trials have been rather limited due to the

¹Department of Pharmacology and Department of Medical Science, College of Medicine, Chungnam National University, 266 Munhwa-ro, Daejeon, 35015, Republic of Korea. ²College of Pharmacy, Chungnam National University, Daejeon, 34134, Republic of Korea. ³Department of Biological Sciences, College of Biosciences and Biotechnology, Chungnam National University, Daejeon, 34134, Republic of Korea. Correspondence and requests for materials should be addressed to M.N. (email: mkna@cnu.ac.kr) or G.M.H. (email: gmmhur@cnu.ac.kr)

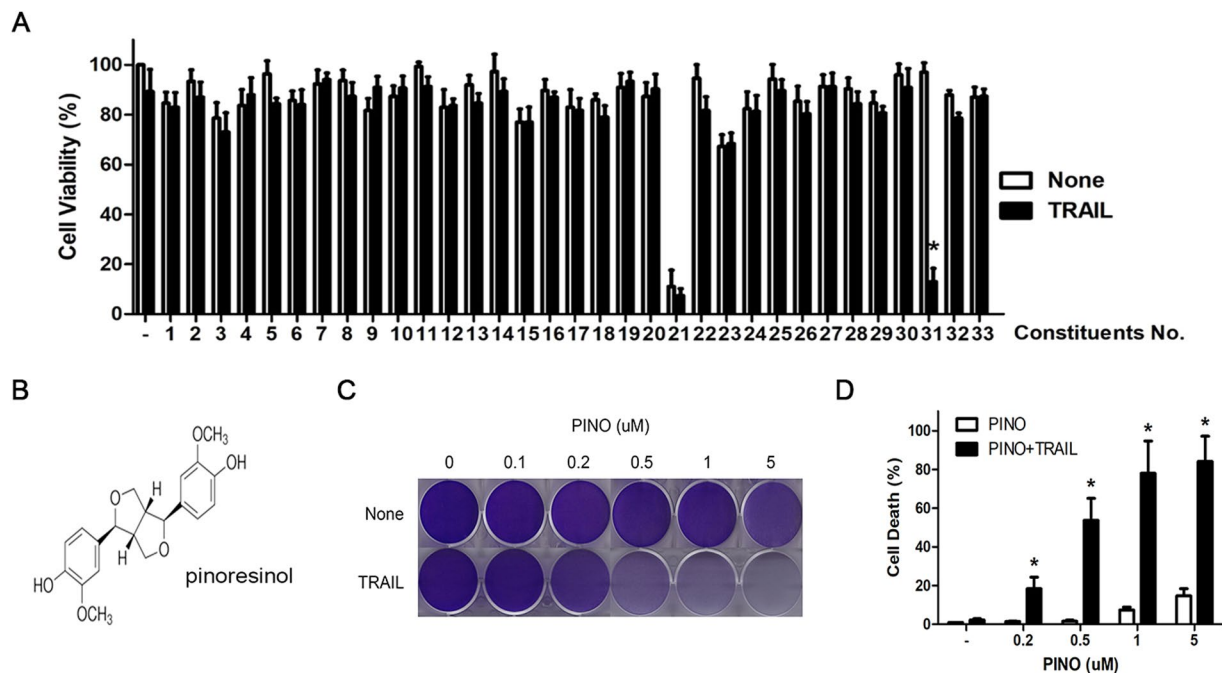


Figure 1. Identification of pinoresinol as a potent TRAIL sensitizer from the constituents of *R. philippinensis*. (A) Screening of the principle constituents of *R. philippinensis* for potential cytotoxic enhancer in TRAIL resistant glioblastoma cells. LN428 cells were pretreated with a series of constituents (5 μM) for 30 min, followed by 50 ng/ml TRAIL for 24 h. Cell death was quantified by using Cell Titer-glo Luminescent cell viability assay kit as described as Methods. (B) Chemical structure of pinoresinol (PINO). (C,D) LN428 cells were pretreated with indicated concentrations of PINO, followed by 50 ng/ml TRAIL. After 24 h, cells were fixed, stained and photographed. (C) Cell death was quantified as in A. (D) Data were normalized to the rate of spontaneous cell death occurring in untreated cells. Data represents the mean ± SE of three independent experiments. Statistical difference (* $p < 0.05$) compared with the PINO only-treated group are indicated.

appearance of cancer cells that escape the cytotoxicity induced by TRAIL-targeted therapy^{11,12}. Thus, the discovery of a therapeutic strategy module that can eradicate cancer cells without restoring resistance has been pending in the field of TRAIL-based chemotherapy.

The genus *Rubia* (family Rubiaceae), a perennial herb, is widely distributed worldwide. It is one of the most attractive plant resources because of its potent and wide spectrum of *in vivo* and *in vitro* biological activities, which include anti-cancer, anti-inflammatory, and anti-angiogenic effects^{13–15}. In a recent phytochemical study of *Rubia philippinensis* Elmer, we isolated several compounds, including derivatives of anthraquinones, pentacyclic triterpenoids, cyclopeptides, and lignans^{16–18}. Although several studies have reported the anti-cancer effects of *Rubia* species, the effects of the principle constituents of *R. philippinensis* on DR-mediated cell death, particularly during TRAIL sensitization, have not yet been determined. As part of our ongoing search to identify potential therapeutic approaches for sensitizing TRAIL-mediated cell death, we tested 33 compounds isolated from *R. philippinensis* and found that nontoxic doses of pinoresinol, a lignan, drastically sensitized cancer cells against TRAIL-induced apoptosis. Pinoresinol facilitated DISC formation to trigger a caspase-8-dependent apoptotic cascade activation in TRAIL-resistant glioblastoma cells. Moreover, our findings revealed novel evidence that the prominent sensitizing effects of pinoresinol against TRAIL-mediated apoptosis involved the downregulation of levels of cellular FLICE-inhibitory protein (cFLIP₁) by a mechanism involving *de novo* protein synthesis.

Results

Identification of pinoresinol from *R. philippinensis* as a TRAIL sensitizer in TRAIL resistant glioma cells. We characterized a set of major compounds obtained from *R. philippinensis* to identify active constituents that synergistically sensitized the cytotoxic effects of TRAIL in TRAIL-resistant glioblastoma cells (Supplementary Table S1, Supplementary Figs 1–33). Treatment of LN428 cells with 50–200 ng/mL TRAIL alone induced a limited number of cell deaths (<5%) over 24 h (data not shown). In the screening assay, LN428 cells were sequentially treated with the purified compounds and 50 ng/mL TRAIL, followed by an ATP-based cell viability assay. In parallel, we tested the cytotoxicity of each compound on LN428 cells as single agents. Of the compounds screened, the lignin pinoresinol was a potent sensitizer of TRAIL-mediated cytotoxicity (Fig. 1A,B). It eliminated the survival of LN428 cells but only in the presence of TRAIL; it had only marginal growth inhibitory effects as a single agent (Fig. 1C). Consistently, no cell death was observed when cells were treated with pinoresinol alone at concentrations up to 1 μM over 24 h. By contrast, combined treatment with the same concentrations of pinoresinol and TRAIL resulted in a drastic increase in cell death (Fig. 1D), thus confirming that this combination resulted in extensive cell death at low concentrations (0.2–1 μM) of pinoresinol.

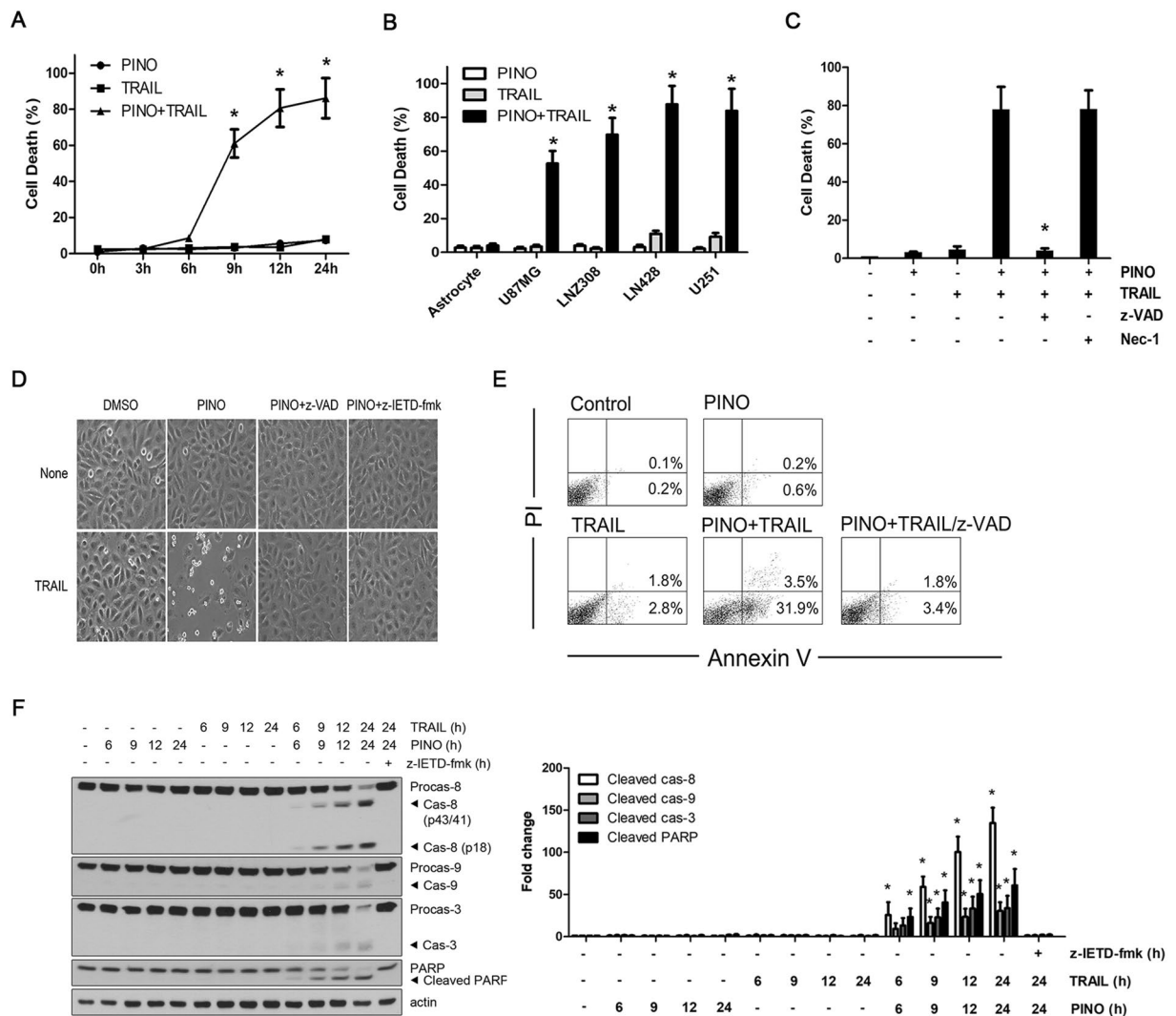


Figure 2. Sensitization of TRAIL-induced apoptosis by non-toxic dose of pinoresinol requires caspase-8 activation in various glioblastoma cells, but not in normal astrocytes. **(A)** LN428 cells were treated with PINO (0.5 μ M), TRAIL (50 ng/ml) and TRAIL (50 ng/ml) plus PINO (0.5 μ M) for the indicated times. **(B)** TRAIL resistant glioblastoma cells (U87MG, LNZ308, LN428, and U251) and normal primary astrocytes were treated with PINO, TRAIL and TRAIL plus PINO for 24 h. Cell death was quantified as in Fig. 1A. Data were normalized to the rate of spontaneous cell death occurring in untreated cells. Data represents the mean \pm SE of three independent experiments. * p < 0.05, compared with the TRAIL only-treated group. **(C,D)** LN428 cells were treated with PINO, TRAIL and TRAIL plus PINO for 24 h in the absence or presence of caspase or necroptosis inhibitor z-VAD-fmk (20 μ M)/z-IETD-fmk (50 μ M) or Nec-1 (30 μ M). **(C)** Cell death was quantified as in A. Data represents the mean \pm SE of three independent experiments. * p < 0.05, compared with the PINO/TRAIL-treated group. **(D)** Cells were visualized using an inverted microscope. **(E)** LN428 cells were treated with PINO, TRAIL and TRAIL plus PINO for 24 h in the absence or presence of z-VAD-fmk. Cells were subjected to Annexin V/PI staining, and then analyzed by flow cytometry. **(F)** LN428 cells were treated with PINO (0.5 μ M), TRAIL (50 ng/ml) and TRAIL plus PINO for indicated times. Whole cell lysates were subjected to immunoblotting with the indicated antibodies (left) and densitometry analysis of the bands from the relevant proteins was performed (right). Data represents the mean \pm SE of three independent experiments. * p < 0.05, compared with the TRAIL only-treated group.

Sensitization of TRAIL-induced killing by pinoresinol is associated with a caspase-8-dependent apoptotic cascade in glioma cells. Next, to validate the above screening results, we performed kinetic experiments to evaluate the synergistic induction of cell death using a nontoxic concentration (0.5 μ M) of pinoresinol. TRAIL-mediated cytotoxicity began to appear from 9 h after pinoresinol co-treatment, and rapidly increased up to 24 h (Fig. 2A). In addition, pinoresinol had a similar synergistic efficacy against TRAIL-mediated cytotoxicity in three other glioblastoma cell lines (U87MG, LNZ308, and U251). By contrast, normal astrocytes were not sensitive to TRAIL-induced killing when treated with pinoresinol (Fig. 2B). These results suggest that the TRAIL-sensitizing effects of pinoresinol might apply to a wide spectrum of glioblastoma cell lines that could

be limited to cancer cells. Although TRAIL-induced cancer cell death was mainly apoptotic, it might also induce non-apoptotic cell death via non-canonical TRAIL signaling depending on the cellular context^{19–21}. Thus, next, we examined whether cell death caused by pinorensinol plus TRAIL was associated with caspase-dependent apoptosis. As expected, pretreatment of LN428 cells with pancaspase and the irreversible caspase 8-inhibitors z-VAD-FMK and z-IETD-fmk completely abrogated the cytotoxicity induced by pinorensinol plus TRAIL (Fig. 2C,D). However, necrostatin-1, an inhibitor of programmed necrosis, failed to protect against cell death, indicating that pinorensinol predominantly triggered apoptotic, rather than necrotic, cell death. To confirm the mode of TRAIL-mediated cell death sensitized by pinorensinol, cell death was analyzed by Annexin V and propidium iodide (PI) staining followed by flow cytometry. Consistently, treatment of pinorensinol plus TRAIL drastically increased the population of an early phase of apoptosis (Annexin V⁺), whereas very few cells were stained exclusively with PI, and such increased apoptotic population was prevented by co-treatment with z-VAD-FMK (Fig. 2E). To get more insights into the mechanisms underlying TRAIL-sensitized apoptosis, we sequentially analyzed the activation of processes of caspase signaling cascade, including those of initiator caspase (caspase-8) and as executor caspases (caspase-3 or -9) and the resultant PARP cleavage. In the kinetic analysis, we found that the treatment of pinorensinol plus TRAIL caused an activation of caspase-8 and -3, and PARP cleavage from 6 h onwards (Fig. 2F). Furthermore, pretreatment with z-IETD-fmk completely inhibited the activation of caspase cascade induced by pinorensinol plus TRAIL treatment. These results clearly indicate that caspase-8 activation is essential in the sensitization of pinorensinol-induced apoptosis in TRAIL-resistant glioblastoma cells.

Sensitizing efficacy of pinorensinol on TRAIL-mediated apoptosis is not associated with either NF- κ B or p53. Pinorensinol exhibits anti-inflammatory properties via blockade of the NF- κ B pathway in several immune and cancer cells^{22–24}. Given the well-established ability of NF- κ B to regulate TRAIL resistance through induction of its anti-apoptotic genes²⁵, it was hypothesized that the anti-NF- κ B effects of pinorensinol might contribute to sensitization against TRAIL-induced apoptosis. Consistent with previous studies^{22–24}, pretreatment of LN428 cells with pinorensinol significantly decreased the transcriptional activity of NF- κ B induced by either TNF or TRAIL, while pinorensinol alone did not affect the basal level of NF- κ B activity (Fig. 3A). However, unexpectedly, LN428 cells with prevention of NF- κ B activation by overexpression of the I κ B α super-repressor (SR-I κ B α), which could not be phosphorylated due to substitutions of serine 32 and serine 36 by alanine, were found to have a similar extent of cell death after TRAIL or pinorensinol plus TRAIL treatment, although TNF-induced cell death was drastically enhanced (Fig. 3B). In addition, pretreatment with the NF- κ B inhibitor TPCA failed to affect cell death upon TRAIL or pinorensinol plus TRAIL treatment (Fig. 3C). These results suggest that the TRAIL-sensitizing efficacy conferred by pinorensinol was unlikely to be a result of NF- κ B inhibition. Although p53 activation plays an important role in TRAIL sensitization^{1,26}, the involvement of p53 in pinorensinol-induced TRAIL sensitization was excluded because LN428 cells retained mutant-p53²⁷. Consistent with this possibility, we found that pinorensinol treatment also sensitized TRAIL-induced cell death in p53 null HCT116 cells to a similar extent as it did with wild type (WT) cells, despite the remarkable differences in cytotoxicity after camptothecin treatment between these two cell types (Fig. 3D). Moreover, no detectable induction of p53 and its target p21 upon pinorensinol alone or pinorensinol plus TRAIL treatment in WT-HCT116 cells, despite the fact that the substantial amounts of p53 and p21 were induced by a DNA damaging agent, camptothecin in WT-HCT116 cells but not in p53- null HCT116 cells (Fig. 3E). Such findings thus indicate that pinorensinol's effect on TRAIL-mediated cell death is independent of p53.

Pinorensinol accelerates DISC formation by down-regulating cFLIP_L expression. To characterize the underlying mechanism involved in pinorensinol-induced sensitization of glioma cells against TRAIL-mediated apoptosis, we determined the expression levels of several apoptosis-related proteins in the death receptor signaling pathway after exposure to pinorensinol for different times in LN428 cells. Notably, the protein expression levels of the long isoform of cellular FLIP (cFLIP_L) and survivin were drastically decreased in a time-dependent manner in LN428 cells with pinorensinol (Fig. 4A, panels 6,7). Reductions of cFLIP_L and survivin were accompanied by increased levels of cleaved-RIP1 and truncated-Bid (t-Bid) in cells upon pinorensinol plus TRAIL treatment (Fig. 4A, panels 4,11). Furthermore, we observed that pinorensinol was also able to down-regulate cFLIP_S expression with a similar kinetics with cFLIP_L in HT-29 cells, though the expression level of cFLIP_S was extremely low or nondetectable in glioblastoma cells including LN428 cells and LN308 cells (Fig. 4B). These results suggest that expression of cFLIP isoforms is highly cell type-specific and pinorensinol-induced cFLIP downregulation, especially in cFLIP_L, may play a predominant role in sensitizing TRAIL-mediated apoptosis in glioblastoma cells. By contrast, the protein levels of signaling components of TRAIL including death receptors, adaptor proteins, other inhibitor of apoptosis proteins, and Bcl-2 family proteins were not affected or only modestly affected in cells after pinorensinol treatment. The expression of cFLIP_L and survivin proteins are regulated by either transcriptional or post-translational modifications such as ubiquitin-mediated proteasomal degradation^{28–31}. In contrast to the observed down-regulation of cFLIP_L and survivin protein levels, treatment with pinorensinol did not change their mRNA levels at any of the time points examined (Fig. 4C). However, pretreatment with the proteasome inhibitor MG132 sufficiently prevented the down-regulation of cFLIP_L and survivin expression by pinorensinol (Fig. 4D), suggesting that pinorensinol might reduce the protein levels of cFLIP_L and survivin via proteasome-mediated degradation rather than through transcriptional control.

Next, we examined whether downregulation of cFLIP_L and survivin by pinorensinol affected the facilitated TRAIL-mediated cytotoxicity by overexpressing these genes in LN428 cells. Consistent with its critical function to antagonize caspase-8, overexpression of WT cFLIP_L resulted in a significant decrease in cell death and caspase cascade activation induced by pinorensinol plus TRAIL treatment (Fig. 5A,B). We also found that a cFLIP_L mutant (cFLIP_L-K167/195R containing modified major ubiquitin acceptor sites) more profoundly abrogated pinorensinol plus TRAIL-induced caspase-dependent apoptosis, compared to that of WT cFLIP_L. However, the cell death

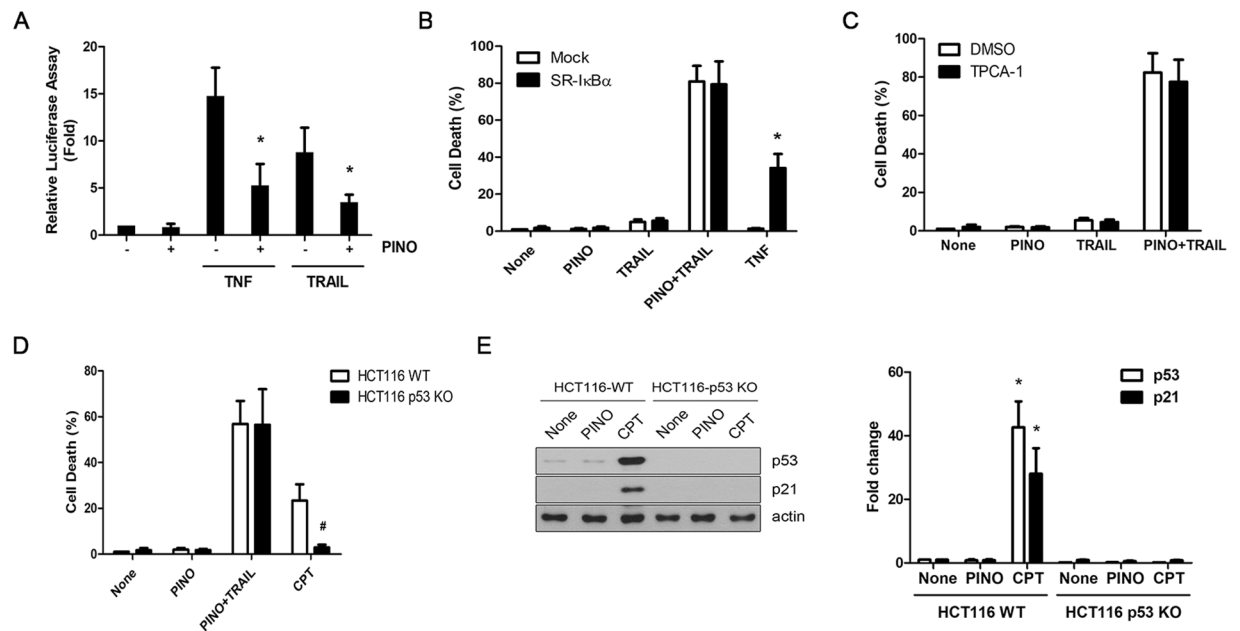


Figure 3. Sensitizing effect of pinoselin against TRAIL-mediated apoptosis is not associated with either NF- κ B or p53 signaling pathway. **(A)** LN428 cells were transfected with an NF- κ B-responsive reporter plasmid (p2xNF-B-Luc) and pRSV- β -gal. After 24 h, cells were treated with PINO (0.5 μ M) alone for 6 h, or pretreated with PINO (0.5 μ M) for 30 min, followed by TNF (30 ng/ml) or TRAIL (50 ng/ml) for additional 6 h. The luciferase assays were performed as describe in Methods, and the activity of each sample was normalized according to β -galactosidase activity. Each column shows the mean \pm SE of three independent experiments. * p < 0.05, compared with the TNF or TRAIL only-treated group. **(B)** LN428 cells were transfected with mock or I κ B α super-repressor (SR-I κ B α) plasmid. After 24 h, cells were treated with PINO, TNF, TRAIL or TRAIL plus PINO for additional 24 h. **(C)** LN428 cells were pretreated with IKK α/β inhibitor TPCA-1 (0.5 μ M) for 30 min, followed by PINO, TRAIL or TRAIL plus PINO for additional 24 h. **(D)** Wild-type and p53 null HCT116 cells were treated with PINO, TRAIL plus PINO and camptothecin (Cpt, 100 μ M) for 24 h. **(B–D)** Cell death was quantified as in Fig. 1A. Data were normalized to the rate of spontaneous cell death occurring in untreated cells. Data represents the mean \pm SE of three independent experiments. * p < 0.05, compared with the mock-transfected group. # p < 0.05, compared with the wild-type HCT116 cells. **(E)** Wild-type and p53 null HCT116 cells were treated with PINO and camptothecin for 24 h. Whole cell lysates were subjected to immunoblotting with the indicated antibodies (left) and densitometry analysis of the bands from the relevant proteins was performed (right). * p < 0.05, compared with the none-treated group.

induced by pinoselin plus TRAIL was not affected by the overexpression of survivin, suggesting that down-regulation of upstream anti-apoptotic protein anti-cFLIP_L, rather than survivin, contributed to an important mechanism involving pinoselin sensitization of TRAIL-induced cell death.

The cFLIP isoforms compete directly with procaspase-8 for binding to FADD in a TRAIL-dependent fashion, thus inhibiting procaspase-8/-10 recruitment to form the DISC^{31,32}. It is therefore possible that downregulation of cFLIP_L by pinoselin might directly affect the formation of the DISC, an early signaling event in TRAIL-induced apoptosis. An immunoprecipitation assay using an anti-caspase-8 antibody revealed that treatment of LN428 cells with TRAIL in the absence of pinoselin led to efficient recruitment of cleaved cFLIP_L to the isolated DISC, whereas DISC-bound FADD and caspase-8/-10 were only weakly detected (Fig. 5C, left panel, rows 1–3). These results suggest that in LN428 cells, the TRAIL-induced recruitment of cFLIP_L into the DISC was an important step before caspase-8 activation to exhibit resistance against TRAIL cytotoxicity. However, pretreatment with pinoselin promoted an increase in TRAIL-mediated DISC formation and procaspase-8/10 processing, concomitant with decreasing amounts of DISC-bound cFLIP_L (Fig. 5C, left panel, rows 4–6). More importantly, in pinoselin-pretreated cells, activation of procaspase-8 processing within the DISC following TRAIL treatment proceeded to completion, as shown by the appearance of the active p18 subunit of mature caspase-8. Taken together, these results strongly suggest that a reduced amount of DISC-bound cFLIP_L played a major role in TRAIL sensitization by pinoselin.

Pinoselin-mediated down-regulation of cFLIP_L is mediated via *de novo* protein synthesis inhibition. Next, we identified the underlying mechanism by which pinoselin directly controls ubiquitin-mediated degradation of cFLIP_L. As expected, co-immunoprecipitation analyses showed that treatment of cells with MG132 led to an increase in polyubiquitinated cFLIP_L with concomitant enhanced protein levels (Fig. 6A). However, we unexpectedly detected lower levels of ubiquitinated cFLIP_L in cells treated with pinoselin plus MG132, compared to cells exposed to MG132 cells, indicating that the accelerated proteasomal degradation of cFLIP_L by pinoselin was not achieved through direct activation of the ubiquitination process.

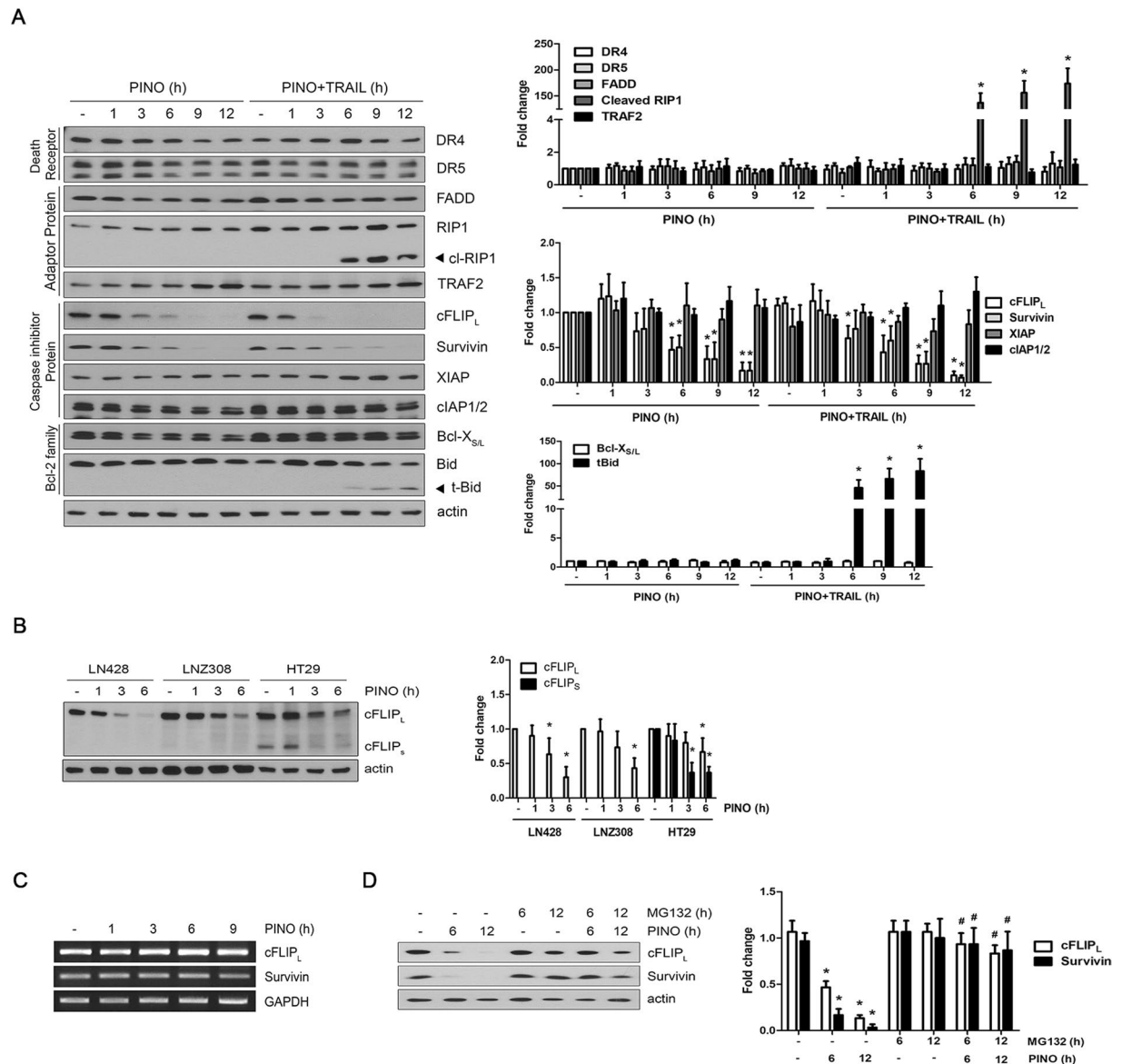


Figure 4. Pinosresinol down-regulates the expression of cFLIP_L and survivin at the post-translational levels via proteasome-mediated degradation. **(A)** LN428 cells were treated with PINO (0.5 μ M) in the absence or presence of TRAIL (50 ng/ml) for the indicated times. **(B)** LN428, LNZ308 and HT29 cells were treated with PINO (0.5 μ M) for the indicated times. Whole cell extracts were subjected to immunoblotting with the indicated antibodies (left). Densitometry analysis of the bands from the relevant proteins was performed (right). Data represents the mean \pm SE of three independent experiments. * p < 0.05, compared with none-treated group. **(C)** Total RNA was prepared at the indicated times after PINO (0.5 μ M) treatment in LN428 cells, and RT-PCR was performed with the primers specific to human cFLIP_L, survivin and GAPDH. After PCR amplification, the products were separated by agarose gel electrophoresis and visualized using ethidium bromide staining. **(D)** LN428 cells were treated with PINO (0.5 μ M) for the indicated times in the absence or presence of proteasome inhibitor MG-132 (10 μ M). Whole cell extracts were subjected to immunoblotting with the indicated antibodies (left), and densitometry analysis of the bands from the relevant proteins was performed (right). Data represents the mean \pm SE of three independent experiments. * p < 0.05, compared with none-treated group. # p < 0.05, compared with PINO only-treated group.

Given that cFLIP_L and survivin are unstable proteins with a rapid turnover^{29,33}, we addressed whether the reduced protein levels by pinosresinol were associated with *de novo* protein synthesis of cFLIP_L and survivin. Treatment with either pinosresinol or cycloheximide (CHX) did not influence the cellular amounts of DRs and adaptor proteins, including DR4/5, FADD, RIP1, and TRAF2 (Fig. 6B). By contrast, pinosresinol was able to down-regulate the expression levels of cFLIP_L and survivin with similar kinetics to that of CHX. Furthermore, the down-regulating effect by either pinosresinol or CHX was not accelerated by the combined treatment of pinosresinol and CHX. These results suggest that in a similar manner to CHX, pinosresinol inhibited *de novo* synthesis of proteins with a rapid turnover cFLIP and survivin.

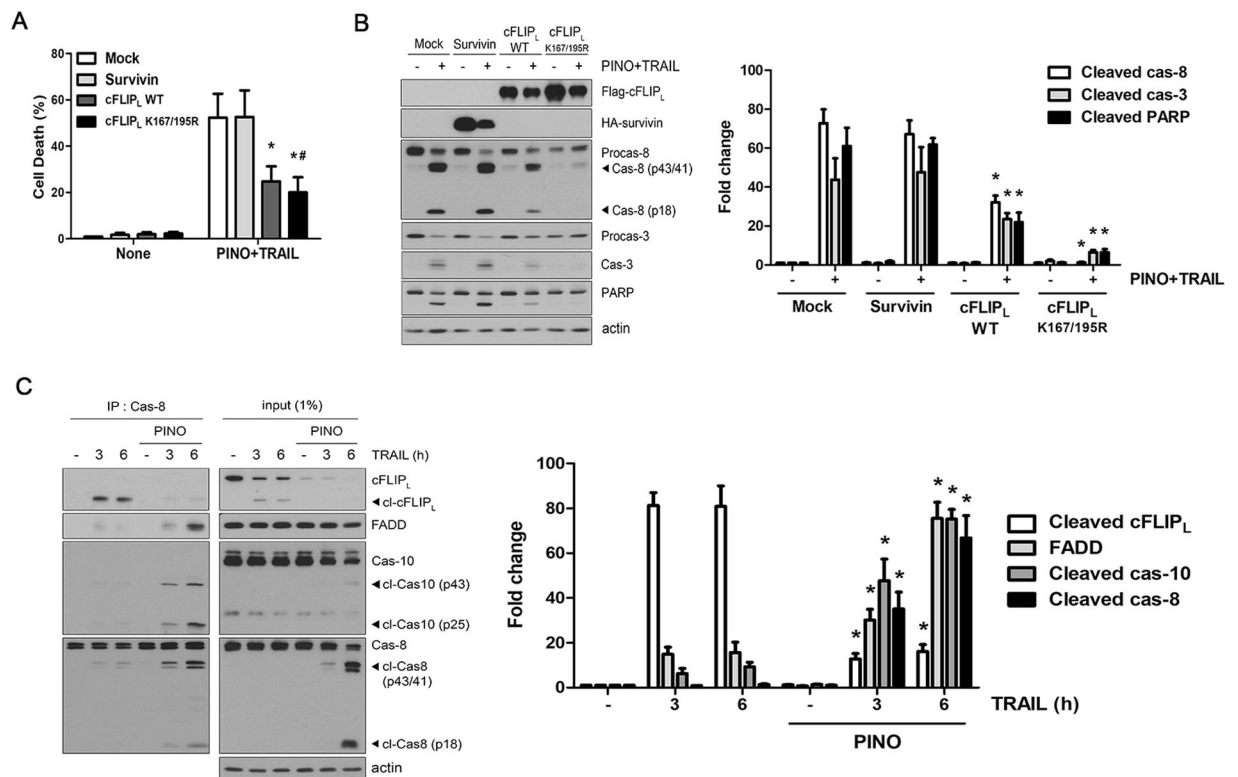


Figure 5. Pinosesin-mediated down-regulation of cFLIP_L accelerates TRAIL DISC formation. (A,B) LN428 cells were transfected with plasmids expressing flag-tagged FLIP_L (wild type; WT or K167/195 R) and WT-survivin plasmids for 24 h, and followed by TRAIL (50 ng/ml) plus PINO (1 μM) for 12 h. (A) Cell death was quantified as in Fig. 1A. Data were normalized to the rate of spontaneous cell death occurring in untreated cells. Data represents the mean ± SE of three independent experiments. **p* < 0.05, compared with the mock-transfected group. #*p* < 0.05, compared with the wild-type FLIP_L-transfected group. (B) Whole cell extracts were subjected to immunoblotting with the indicated antibodies (left), and densitometry analysis of the bands from the relevant proteins was performed (right). Data represents the mean ± SE of three independent experiments. **p* < 0.05, compared with mock-transfected group. (C) LN428 cells were treated with TRAIL (50 ng/ml) in the absence or presence of PINO (0.5 μM) for the indicated times. Cell extracts from each sample were subjected to immunoprecipitation with anti-caspase-8 antibody. Immunoprecipitants were analyzed by immunoblotting with indicated antibodies. A total of 1% of the cell extract volume from each sample was used as input control (left). Densitometry analysis of the bands from the relevant proteins was performed (right). Data represents the mean ± SE of three independent experiments. **p* < 0.05, compared with none-treated group.

To directly assess whether the down-regulation of protein expression by pinosresinol is due to the impairment of the general translational machinery, we conducted a cell-free *in vitro* transcription and translation assay. As shown in Fig. 6C, pinosresinol suppressed the production of green fluorescent protein (GFP), similar to a well-known protein translation inhibitor CHX, in a dosage dependent manner. To rule out the possibility that pinosresinol-dependent suppression of protein synthesis is caused by hampering transcriptional processes, subsequent *in vitro* translation response was assessed by using *in vitro* synthesized EGFP mRNA. Consistently, incubation with 1 μM pinosresinol completely interfered the EGFP protein production with a similar efficacy of 10 μM CHX (Fig. 6D). Taken together, these data indicate that pinosresinol directly interferes a *de novo* protein synthesis without affecting transcriptional machinery.

Discussion

Glioblastoma is a heterogenous group of invasive malignant primary brain tumors with high mortality³⁴. Although all populations of cancer cells contribute in their own way to drive tumor growth, the molecular changes disrupting the apoptotic pathway are considered a pathological hallmark of glioblastoma. Emerging evidence suggests that cells within the glioblastoma exhibit abnormalities of the cell death pathway such as over-expression of antiapoptotic proteins or silencing of key death effectors^{35,36}. Importantly, genomic analyses of human glioblastomas have shown that caspase-8, an essential component of the DISC, is frequently inactivated by either gene mutations or promotor methylation^{7,37–39}. Thus, resistance to DR-mediated cytotoxicity in glioblastoma cells might occur as a step of DISC assembly. Consistent with this possibility, we found that in a series of glioblastoma cells including LN428 cells treated with TRAIL, complete activation of caspase-8 and functional DISC formation were blocked. However, pinosresinol treatment resulted in cells resistant to apoptosis with an

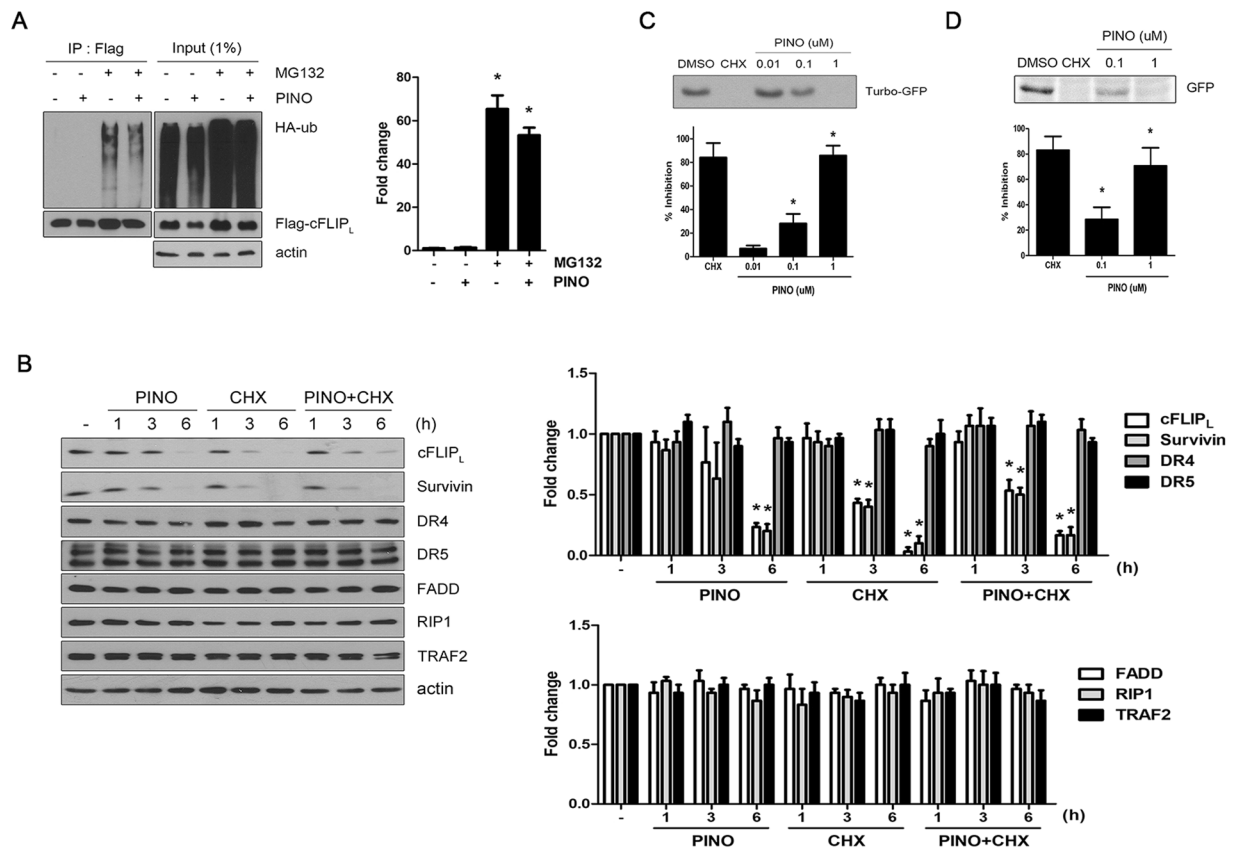


Figure 6. Pinoresinol-induced down-regulation of cFLIP_L is mediated via *de novo* protein synthesis inhibition. **(A)** LN428 cells were co-transfected with plasmids expressing flag-tagged cFLIP_L and HA-tagged ubiquitin plasmids for 24 h. The cells were then treated with PINO (0.5 μM) for 4 h in the absence or presence of MG-132 (10 μM). Cell extracts from each sample were subjected to immunoprecipitation with anti-flag antibody followed by immunoblotting with anti-HA antibody for detection of ubiquitinated cFLIP_L. A total of 1% of the cell extract volume from each sample was used as input control (left). Densitometry analysis of the bands from the relevant proteins was performed (right). Data represents the mean ± SE of three independent experiments. **p* < 0.05, compared with none-treated group. **(B)** LN428 cells were treated with PINO (0.5 μM), cycloheximide (CHX, 10 μM) and PINO (0.5 μM) plus CHX (10 μM) for indicated times. Whole cell extracts were subjected to immunoblotting with the indicated antibodies (left). Densitometry analysis of the bands from the relevant proteins was performed (right). Data represents the mean ± SE of three independent experiments. **p* < 0.05, compared with none-treated group. **(C)** The *in vitro* coupled transcription and translation assay was performed using 1-Step Human Coupled IVT Kit as described in Methods. pCFE-GFP plasmid as template in HeLa cell lysate supplemented with indicated concentrations of CHX and PINO. **(D)** *In vitro* translation inhibition assay with increased amount of PINO. *In vitro* transcribed mRNA encoding EGFP was purified as described in Methods. 3 μg of EGFP mRNA each in HeLa cell lysate was incubated for 6 h with indicated concentrations of CHX and PINO. The *in vitro* translation yield of EGFP protein was monitored by immunoblotting with anti-Turbo GFP or anti-GFP antibody, respectively and quantified using a densitometry from the relevant proteins (top). Percent inhibition of protein synthesis was calculated by dividing the band intensities from each concentration of PINO over control DMSO-treated samples (bottom).

increased recruitment of both procaspase-8 and FADD to the TRAIL DISC, and complete activation of caspase-8. It is therefore possible that pinoresinol-induced TRAIL sensitization was conducted at the level of the DISC/caspase-8 axis.

Accumulating evidence presently suggests that cFLIP is a key player in the DR-mediated apoptotic pathway that retains the sublethal activation of caspase-8 at the DISC^{31,32,40}. Consequently, elevated levels of cFLIP in tumor tissues from patients with a variety of cancers including lung cancer, Burkitt's lymphoma, cervical carcinoma and colorectal carcinoma are correlated with poor clinical outcomes^{41–44}, implicating the existence of a strong association between suppression of DISC-mediated apoptosis by cFLIP and tumorigenesis. An important finding from the present study is that protein levels of cFLIP_L were significantly reduced by pinoresinol treatment, and the ectopic overexpression of cFLIP_L, significantly suppressed caspase-8 activation and reduced the susceptibility to cell death caused by pinoresinol/TRAIL treatment in LN428 cells. Changes in the expression levels of cFLIP_L by pinoresinol therefore appear to be responsible for TRAIL sensitization in glioma cells. In this regard, it is important to determine the potential mechanism involved in the pinoresinol-induced downregulation of

cFLIP_L expression. It has previously been reported that cFLIP_L expression is tightly regulated at the transcriptional level by a number of stimuli, including NF- κ B transcription factor^{45,46}, mitogen-activated protein kinase⁴⁷ and protein kinase B/Akt^{48,49}. Previous pharmacological and biochemical studies have reported that pinoselinol exhibits anti-inflammatory and anti-cancer effects, in part through the inhibition of NF- κ B^{22–24}. It is therefore possible that pinoselinol suppresses cFLIP_L expression through NF- κ B inhibition. In accordance with previous observations, we found that pinoselinol potentially inhibited the NF- κ B activity in LN428 cells in response to TNF and TRAIL. However, we did not observe a decrease in cFLIP_L mRNA expression levels in cells treated with pinoselinol concentrations of 0.5–1 μ M, which caused cFLIP_L depletion and maximal TRAIL sensitization. Furthermore, the expressions of a subset of NF- κ B-inducible genes, including *TRAF2*, *cIAP1/2*, *XIAP*, and *Bcl-X_L*, were unaffected by pinoselinol treatment. These findings raise the possibility that down-regulatory effects of pinoselinol on cFLIP_L expression are not associated with transcriptional regulation of NF- κ B. These discrepancies of transcriptional regulation between cFLIP_L expression and NF- κ B may have resulted from different concentrations of pinoselinol. Indeed, pinoselinol must be used at a relatively high concentration ($\geq 10 \mu$ M) to exhibit anti-NF- κ B activity in several types of cells^{22,23,50}, suggesting that other factors may be involved in the effects of cFLIP_L depletion by low concentrations of pinoselinol.

On the other hand, the expression levels of cFLIP_L were regulated by the ubiquitin–proteasomal pathway with a short half-life^{29,51}. In this respect, it is of particular interest that, in LN428 cells, pinoselinol induces proteasomal degradation of cFLIP_L or ectopic expression of the cFLIP_L mutant (cFLIP_L-K167/195 R), which significantly abolishes sensitization by pinoselinol to TRAIL-induced cytotoxicity. Furthermore, the results of an *in vitro* translational assay showed that pinoselinol directly inhibited *de novo* protein synthesis, which has similar efficiency with the well-known protein synthesis inhibitor CHX. These results raise the possibility that pinoselinol disrupts *de novo* protein synthesis, particularly for fast turnover proteins such as cFLIP_L, leading to proteasomal degradation with decreased stability. Nevertheless, it is currently unclear how pinoselinol inhibits *de novo* protein synthesis. Further studies to identify the ribosomal proteins that interact with pinoselinol in the translational machinery will be critical for a complete understanding of the mechanism of action, and for the development of novel TRAIL-based chemotherapies. Earlier, it has been reported that survivin plays an essential role in cell cycle progression⁵². In this study, we found that pinoselinol induced a G2/M arrest with an increase in the G2 population (Supplementary Fig. 34), suggesting that down regulation of survivin by pinoselinol might be relevant in limiting cell division, especially in G2-M phase rather than apoptosis. In addition, it has recently been reported that pinoselinol suppresses the efflux of chemotherapeutic drugs outside by interacting with P-glycoprotein (P-gp) encoded by multidrug resistant-1 (MDR-1) gene^{53,54}. Since P-gp efflux function was shown to contribute to TRAIL resistance via controlling the endogenous level of TRAIL in certain types of cancer cells^{55,56}, such an anti-Pgp activity of pinoselinol might constitute another mechanism in enhancing TRAIL efficacy in TRAIL-resistant cancers including glioblastoma. Thus, future bioavailability study of TRAIL and pinoselinol using *in vivo* preclinical models are required to further validate TRAIL and pinoselinol-based therapeutic development for glioblastoma.

Methods

Isolation of pinoselinol. Pinoselinol was isolated from our chemical study on *Rubia philippinensis*, as described previously¹⁷. Briefly, a methylene chloride (CH₂Cl₂)-soluble fraction (50 g) was prepared from solvent extraction of *R. philippinensis* extract (150 g) using CH₂Cl₂ and water. Vacuum liquid chromatography of CH₂Cl₂-soluble fraction on silica gel column (20 \times 20 cm) eluting with *n*-hexanes-EtOAc (20:1, 10:1, 5:1, 3:1, 2:1) and CHCl₃-MeOH (8:1) resulted in the preparation of six column fractions (D-1 \rightarrow D-6). Fraction D-6 (10 g) was separated by reversed-phase C18 column chromatography [column: SNAP cartridge KP-C18-HS (400 g), mobile phase: MeOH-H₂O (10:90 \rightarrow 100:0, 7 L)] and 11 subfractions (D-6-1 \rightarrow D-6-11) were obtained. Pinoselinol (*t_R* 34.0 min, 40 mg) was purified from D-6-4 (360 mg) by preparative HPLC [column: Phenomenex C₁₈ (250 \times 21.2 mm), mobile phase: MeOH-H₂O (50:50, 4 mL/min)]. Pinoselinol: brownish amorphous powder; ESIMS *m/z* 359.2 [M + H]⁺, 381.1 [M + Na]⁺, 357.1 [M - H]⁻, 393.1 [M + Cl]⁻; ¹H NMR (300 MHz, methanol-*d*₄): 3.13 (2H, m, H-8, H-8'), 3.80 (2H, Ha-9, Ha-9'), 3.85 (6H, s, OCH₃-3, OCH₃-3'), 4.22 (2H, Hb-9, Hb-9'), 4.70 (2H, d, *J* = 2.7, H-7, H-7'), 6.77 (2H, overlapped, H-5, H-5'), 6.79 (2H, overlapped, H-6, H-6'), 6.95 (2H, H-2, H-2'), ¹³C NMR (75 MHz, methanol-*d*₄): 133.8 (C-1, C-1'), 111.0 (C-2, C-2'), 149.1 (C-3, C-3'), 147.3 (C-4, C-4'), 116.1 (C-5, C-5'), 120.0 (C-6, C-6'), 87.5 (C-7, C-7'), 55.3 (C-8, C-8'), 72.6 (C-9, C-9'), 56.4 (OCH₃-3, OCH₃-3').

Structure determination of pinoselinol. The molecular formula of purified compound was deduced as C₂₀H₂₂O₆ based on the ESIMS protonated ion at *m/z* 359.2, the sodium-adduct ion at *m/z* 381.1, the deprotonated ion at *m/z* 357.1, and the chloride-adduct ion at *m/z* 393.1 (calcd. for C₂₀H₂₂O₆, *m/z* 358.1). The ¹H NMR data displayed a pair of symmetric benzene ring system at δ_{H} 6.77 (2H, overlapped, H-5, H-5'), 6.79 (2H, overlapped, H-6, H-6'), 6.95 (2H, H-2, H-2'). The proton signals at δ_{H} 3.13 (2H, m, H-8, H-8'), 3.80 (2H, Ha-9, Ha-9'), 4.22 (2H, Hb-9, Hb-9'), 4.70 (2H, d, *J* = 2.7, H-7, H-7') indicated two symmetrical tetrahydrofuran substructure of lignan. In the ¹³C NMR spectroscopic data, six benzene signals at δ_{C} 111.0–149.1, two oxygenated carbons at δ_{C} 87.5 and 72.6, one methine at δ_{C} 55.3, and a methoxy group at δ_{C} 56.4 supported the symmetric structure of tetrahydrofuran-type lignan. The chemical structure was identified as pinoselinol by NMR spectroscopic and LC-MS data analyses⁵⁷.

Antibodies and chemicals. The antibodies and chemicals were obtained from the following resources; anti-PARP (#556362), anti-XIAP (#610716), anti-FADD (#610399), anti-RIP1 (#610459), anti-p53 (#554147) and anti-p21 (#556430) antibodies (BD Biosciences, San Diego, CA, USA); anti-caspase-3 (#9662), anti-caspase-8 (#9746), anti-caspase-9 (#9508) and anti-Bid (#2002) antibodies (Cell signalling Technology, Beverly, MA, USA); anti-caspase-10 (M059-3) antibody (MBL, WOBURN, MA, USA); anti-Bcl-X_{S/L} (sc-271121), anti-survivin

(sc-17779), anti-TRAF2 (sc-876), anti-GFP (sc-9996) and anti-HA (sc-805) antibodies (Santa Cruz, CA, USA); anti-c-FLIP (ALX-804-961) antibody (Enzo Life Sciences, Farmingdale, NY, USA); anti-cIAP1/2 (#07-759) antibody (Upstate Biotech, Waltham, MA, USA); anti-DR5 (#ab181846) antibody (Abcam, Cambridge, UK); anti-DR4 (NB100-56528) antibody (Novus, Centennial, CO, USA); anti-TurboGFP (PA5-22688) antibody (Thermo scientific, Waltham, Massachusetts, USA); anti-actin (A2066), anti-flag (F3165, 1:2,000 dilution) antibodies (Sigma-Aldrich, St. Louis, MO, USA). the pan caspase inhibitor Z-VAD-FMK, MG-132, TPCA-1 (Calbiochem, San Diego, CA, USA); recombinant TNF (R & D Systems, Minneapolis, MN, USA); recombinant human TRAIL/Apo2 ligand (Peptide, Rocky Hill, NJ, USA).

Cell culture and primary astrocytes preparation. Human malignant glioblastoma cells (LN428, LN2308, U87MG, and U251MG) were kindly provided by Dr. Yongwan Kim (Dongsung Cancer Center, Daegu, Korea). HCT 116, a human colorectal cancer cells and its p53-knockout derivatives were kindly provided by Dr. Deug Y. Shin (Dankook University, Cheonan, Korea). Cells were cultured in Dulbecco's modified Eagle's medium (DMEM) including 10% fetal bovine serum, 2 mmol/L glutamine and 100 U/mL penicillin/streptomycin. The normal primary astrocytes were prepared from the neonatal rats, as described previously⁵⁸, and cultured in Minimum Essential Media (MEM) with 10% FBS, 2 mmol/L glutamine and 100 U/mL penicillin/ streptomycin.

Plasmids, transfection and luciferase assay. The expression plasmids of survivin (pCA-flag-survivin) and cFLIP_L (pCA-flag- cFLIP_L) were gift from Dr. Taeg K. Kwon (Keimyung University, Daegu, Korea). The point-mutant of cFLIP_L at lysine 167/195 (cFLIP_L-K167/195 R) was generated by a QuickchangeTM Site-Directed Mutagenesis kit as previously described⁵⁹. For luciferase assay, LN428 cells were transiently co-transfected with p2xNF-kB-Luc and pRSV-β-galactosidase into 1×10^6 cells per well in 6-well plates for 24 h using Lipofectamine reagent (Invitrogen). Cell were then treated with TNF (30 ng/ml) or TRAIL (50 ng/ml) for an additional 6 h, and the luciferase activities were measured using a luciferase assay kit (Promega, Madison, CA, USA) according to the manufacturer's instructions. Luciferase activity obtained were normalized to β-galactosidase activity of each sample.

Cell death assessment. Cell death was determined using Cell Titer-glo Luminescent Cell Viability Assay kit (Promega Co., Fitchburg, WI, USA), according to the manufacturer's instructions. Luminescent signals were measured by Tecan Infinite Plate reader (Tecan group Ltd., Männedorf, Switzerland), and Viability rates were calculated following the formula: viability rates = $(1 - \text{medicating/control}) \times 100\%$. Representative images were also taken by an inverted microscope.

Flow cytometry analysis. After LN428 cells were treated with pinoresinol, as described in the figure legends, the cells were harvested and examined for the mode of apoptotic and necrotic cell death by double staining with FITC-conjugated annexin V and propidium iodide (PI) in 10 mM HEPES buffer, pH 7.4, according to the manufacturer's instructions (BD FITC Annexin V kit). For cell cycle analysis, cells were suspended with ice-cold phosphate buffered saline (PBS) and fixed in 70% ethanol. Cells were washed with PBS and added 100 μg/ml PI solution including 50 μg/ml RNase in PBS for 30 min at room temperature. The cells were analyzed with a FACScan flow cytometer (BD Biosciences).

Immunoblotting and immunoprecipitation. Upon treatment, cells were lysed in ice-cold M2 buffer (20 mM Tris, pH 7.6, 0.5% NP-40, 250 mM NaCl, 3 mM EDTA, 3 mM EGTA, 2 mM dithiothreitol, 0.5 mM PMSF, 20 mM β-glycerol phosphate, 1 mM sodium vanadate, and 1 μg/ml leupeptin). For immunoblot analysis, cell lysates were resolved on 8–12% SDS-polyacrylamide gel (PAGE), transferred onto the PVDF membrane (GE Healthcare Life Sciences). Membranes were serially incubated with specific primary antibodies (1:1,000 dilution) and secondary antibody (1:2,000 dilution), and immunoblots were visualized by enhanced chemiluminescence (ECL) kit (EMD Millipore). For immunoprecipitation assays, the cell lysates were incubated with anti-caspase-8 antibody and protein A-agarose beads at 4 °C overnight. The immunoprecipitants were washed three times with M2 buffer and analyzed by immunoblotting.

RT-PCR analysis. Total RNA was isolated using a ReliaPrep RNA Miniprep kit (Promega), and cDNA was prepared using a M-MLV reverse transcriptase (Promega), according to the manufacturer's instructions. PCR amplification was carried out using the primer pairs specific to each human genes (cFLIP_L, 5'-CTGGTTGCCCCAGATCAACT-3' and 5'-CCCAGGGAAGTGAAGGTGTC-3'; Survivin, 5'-TGACGACCCCATAGAGGAACA-3' and 5'-TCAATCCATGGCAGCCAGC-3'; GAPDH, 5'-CACCATCTTCCAGGAGCGAG-3' and 5'-GATGGCATGGACTGTGGTCA-3').

In vitro translation analysis. *In vitro* coupled transcription and translation analysis was performed with the 1-Step Human Coupled IVT Kit ± DNA (ThermoFisher Scientific) following the manufacturer's instructions. Briefly, the translation reaction was assembled with pre-incubation of HeLa cell lysates with 1 μg of circular DNA (pCFE-GFP) as a template. The reaction mixtures were incubated for 12 hours at 30 °C and were stopped with loading buffer for SDS-PAGE. The expression levels of EGFP proteins were examined by immunoblot analysis using anti-TurboGFP antibody. For *in vitro* translational analysis, EGFP mRNA was synthesized after digesting pcGlobin2-EGFP with XhoI, as described previously⁶⁰. Synthetic EGFP mRNA was generated by using a mMES-SAGE mMACHINE T7 Transcription kit (ThermoFisher Scientific) following manufacturer's instructions. Each 3 μg of purified EGFP mRNA was incubated with HeLa cell lysates for 6 hours at 30 °C with indicated concentrations of PINO and CHX as described in figure legends. The expression level of EGFP was measured through immunoblotting with anti-GFP antibody and then quantified by densitometry using an image J software.

Statistical analysis. Data are expressed as the mean \pm S.E. from at least three separate experiments performed triplicate. Statistical analysis was performed using one-way analysis of variance (ANOVA), followed by the Bonferroni *t*-test for multi-group comparison tests. Student's *t*-test was used to compare the mean values from the two groups. $P < 0.05$ was considered as statistically significant.

References

- Kretz, A. L. *et al.* TRAILblazing Strategies for Cancer Treatment. *Cancers (Basel)* **11**, 456 (2019).
- Sessler, T., Healy, S., Samali, A. & Szegezdi, E. Structural determinants of DISC function: new insights into death receptor-mediated apoptosis signalling. *Pharmacol Ther* **140**, 186–99 (2013).
- Tummers, B. & Green, D. R. Caspase-8: regulating life and death. *Immunol Rev* **277**, 76–89 (2017).
- Feltham, R., Vince, J. E. & Lawlor, K. E. Caspase-8: not so silently deadly. *Clin Transl Immunology* **6**, e124 (2017).
- Bin, L. *et al.* Tumor-derived mutations in the TRAIL receptor DR5 inhibit TRAIL signaling through the DR4 receptor by competing for ligand binding. *J Biol Chem* **282**, 28189–28194 (2007).
- Yu, R. *et al.* DR4 specific TRAIL variants are more efficacious than wild-type TRAIL in pancreatic cancer. *Cancer Biol Ther* **15**, 1658–1666 (2014).
- Li, M. *et al.* Q482H mutation of procaspase-8 in acute myeloid leukemia abolishes caspase-8-mediated apoptosis by impairing procaspase-8 dimerization. *Biochem Biophys Res Commun* **495**, 1376–1382 (2018).
- Finnberg, N., Klein-Szanto, A. J. & El-Deiry, W. S. TRAIL-R deficiency in mice promotes susceptibility to chronic inflammation and tumorigenesis. *J Clin Invest* **118**, 111–123 (2008).
- Fulda, S. Safety and tolerability of TRAIL receptor agonists in cancer treatment. *Eur J Clin Pharmacol* **71**, 525–527 (2015).
- Wajant, H. Molecular Mode of Action of TRAIL Receptor Agonists-Common Principles and Their Translational Exploitation. *Cancers (Basel)* **11**, 954 (2019).
- von Karstedt, S., Montinaro, A. & Walczak, H. Exploring the TRAILs less travelled: TRAIL in cancer biology and therapy. *Nat Rev Cancer* **17**, 352–366 (2017).
- Yuan, X. *et al.* Developing TRAIL/TRAIL death receptor-based cancer therapies. *Cancer Metastasis Rev* **37**, 733–748 (2018).
- Xu, K. *et al.* Structural and bioactive studies of terpenes and cycllopeptides from the Genus *Rubia*. *Chem Cent J* **7**, 81 (2013).
- Do, M. T., Hwang, Y. P., Kim, H. G., Na, M. & Jeong, H. G. Mollugin inhibits proliferation and induces apoptosis by suppressing fatty acid synthase in HER2-overexpressing cancer cells. *J Cell Physiol* **228**, 1087–1097 (2013).
- Gong, X. P. *et al.* Anti-diarrheal and anti-inflammatory activities of aqueous extract of the aerial part of *Rubia cordifolia*. *BMC Complement Altern Med* **17**, 20 (2017).
- An, Y. *et al.* Activation of the p53 pathway with digiferrol isolated from *Rubiaphilippinensis* induces cell cycle arrest, apoptosis, and autophagy in colon cancer cells. *Food Chem Toxicol* **118**, 514–522 (2018).
- Bajpai, V. K. *et al.* Cytotoxic properties of the anthraquinone derivatives isolated from the roots of *Rubia philippinensis*. *BMC Complement Altern Med* **18**, 200 (2018).
- Oh, J. *et al.* NMR-Based Investigation of Hydrogen Bonding in a Dihydroanthracen-1(4H)one from *Rubia philippinensis* and Its Soluble Epoxide Hydrolase Inhibitory Potential. *J Nat Prod* **81**, 2429–2435 (2018).
- He, W. *et al.* Attenuation of TNFSF10/TRAIL-induced apoptosis by an autophagic survival pathway involving TRAF2- and RIPK1/RIP1-mediated MAPK8/JNK activation. *Autophagy* **8**, 1811–1821 (2012).
- Aziji, K., Weyhenmeyer, B., Peters, G. J., de Jong, S. & Kruyt, F. A. Non-canonical kinase signaling by the death ligand TRAIL in cancer cells: discord in the death receptor family. *Cell Death Differ* **20**, 858–868 (2013).
- Yang, M. *et al.* Poly-ADP-ribosylation of HMGB1 regulates TNFSF10/TRAIL resistance through autophagy. *Autophagy* **11**, 214–224 (2015).
- Jung, H. W. *et al.* Pinoselinol from the fruits of *Forsythia koreana* inhibits inflammatory responses in LPS-activated microglia. *Neurosci Lett* **480**, 215–220 (2010).
- During, A., Debouche, C., Raas, T. & Larondelle, Y. Among plant lignans, pinoselinol has the strongest antiinflammatory properties in human intestinal Caco-2 cells. *J Nutr* **142**, 1798–1805 (2012).
- Lin, B. *et al.* Anti-inflammatory constituents from the root of *Litsea cubeba* in LPS-induced RAW 264.7 macrophages. *Pharm Biol* **54**, 1741–1747 (2016).
- Zhang, L. & Fang, B. Mechanisms of resistance to TRAIL-induced apoptosis in cancer. *Cancer Gene Ther* **12**, 228–237 (2005).
- Zhao, J., Lu, Y. & Shen, H. M. Targeting p53 as a therapeutic strategy in sensitizing TRAIL-induced apoptosis in cancer cells. *Cancer Lett* **314**, 8–23 (2012).
- Tabuchi, K., Fukuyama, K., Mineta, T., Oh-Uchida, M. & Hori, K. Altered structure and expression of the p53 gene in human neuroepithelial tumors. *Neurol Med Chir* **32**, 725–732 (1992).
- Martin-Pérez, R., Niwa, M. & López-Rivas, A. ER stress sensitizes cells to TRAIL through down-regulation of FLIP and Mcl-1 and PERK-dependent up-regulation of TRAIL-R2. *Apoptosis* **17**, 349–363 (2012).
- Poukkula, M. *et al.* Rapid turnover of c-FLIPshort is determined by its unique C-terminal tail. *J Biol Chem* **280**, 27345–27355 (2005).
- Pahlavan, Y. *et al.* Survivin modulatory role in autoimmune and autoinflammatory diseases. *J Cell Physiol* **234**, 19440–19450 (2019).
- Humphreys, L., Espona-Fiedler, M. & Longley, D. B. FLIP as a therapeutic target in cancer. *FEBS J* **285**, 4104–4123 (2018).
- Kang, K., Lee, S. R., Piao, X. & Hur, G. M. Post-translational modification of the death receptor complex as a potential therapeutic target in cancer. *Arch Pharm Res* **42**, 76–87 (2019).
- Nogueira-Ferreira, R., Vitorino, R., Ferreira-Pinto, M. J., Ferreira, R. & Henriques-Coelho, T. Exploring the role of post-translational modifications on protein-protein interactions with survivin. *Arch Biochem Biophys* **538**, 64–70 (2013).
- Cai, X. & Sughrue, M. E. Glioblastoma: new therapeutic strategies to address cellular and genomic complexity. *Oncotarget* **9**, 9540–9554 (2017).
- Eisele, G. & Weller, M. Targeting apoptosis pathways in glioblastoma. *Cancer Lett* **332**, 335–345 (2013).
- Fulda, S. Cell death-based treatment of glioblastoma. *Cell Death Dis* **9**, 121 (2018).
- Martinez, R. *et al.* CpG island promoter hypermethylation of the pro-apoptotic gene caspase-8 is a common hallmark of relapsed glioblastoma multiforme. *Carcinogenesis* **28**, 1264–1268 (2007).
- Hervouet, E., Vallette, F. M. & Cartron, P. F. Impact of the DNA methyltransferases expression on the methylation status of apoptosis-associated genes in glioblastoma multiforme. *Cell Death Dis* **1**, e8 (2010).
- Liccardi, G. *et al.* RIPK1 and Caspase-8 Ensure Chromosome Stability Independently of Their Role in Cell Death and Inflammation. *Mol Cell* **73**, 413–428 (2019).
- Tsuchiya, Y., Nakabayashi, O. & Nakano, H. FLIP the Switch: Regulation of Apoptosis and Necroptosis by cFLIP. *Int J Mol Sci* **16**, 30321–30341 (2015).
- Valnet-Rabier, M. B. *et al.* c-Flip protein expression in Burkitt's lymphomas is associated with a poor clinical outcome. *Br J Haematol* **128**, 767–773 (2005).
- Yao, Q. *et al.* Prognostic significance of TRAIL signalling molecules in cervical squamous cell carcinoma. *J Clin Pathol* **69**, 122–127 (2016).
- Ullenhag, G. J. *et al.* Overexpression of FLIPL is an independent marker of poor prognosis in colorectal cancer patients. *Clin Cancer Res* **13**, 5070–5075 (2007).

44. Hutchinson, R. A. *et al.* IHC-based subcellular quantification provides new insights into prognostic relevance of FLIP and procaspase-8 in non-small-cell lung cancer. *Cell Death Discov* **3**, 17050 (2017).
45. Micheau, O., Lens, S., Gaide, O., Alevizopoulos, K. & Tschopp, J. NF-kappaB signals induce the expression of c-FLIP. *Mol Cell Biol* **21**, 5299–5305 (2001).
46. Gordy, C., Liang, J., Pua, H. & He, Y. W. c-FLIP protects eosinophils from TNF- α -mediated cell death *in vivo*. *PLoS One* **9**, e107724 (2014).
47. Marques-Fernandez, F. *et al.* TNF α induces survival through the FLIP-L-dependent activation of the MAPK/ERK pathway. *Cell Death Dis* **4**, e493 (2013).
48. Skurk, C. *et al.* The Akt-regulated forkhead transcription factor FOXO3a controls endothelial cell viability through modulation of the caspase-8 inhibitor FLIP. *J Biol Chem* **279**, 1513–1525 (2004).
49. Wang, X. *et al.* Akt-mediated eminent expression of c-FLIP and Mcl-1 confers acquired resistance to TRAIL-induced cytotoxicity to lung cancer cells. *Mol Cancer Ther* **7**, 1156–1163 (2008).
50. Mitsuhashi, S., Kishimoto, T., Uraki, Y., Okamoto, T. & Ubukata, M. Low molecular weight lignin suppresses activation of NF-kappaB and HIV-1 promoter. *Bioorg Med Chem* **16**, 2645–2650 (2008).
51. Sayers, T. J. V. *et al.* The proteasome inhibitor PS-341 sensitizes neoplastic cells to TRAIL-mediated apoptosis by reducing levels of c-FLIP. *Blood* **102**, 303–310 (2003).
52. Mita, A. C., Mita, M. M., Nawrocki, S. T. & Giles, F. J. Survivin: key regulator of mitosis and apoptosis and novel target for cancer therapeutics. *Clin Cancer Res* **14**, 5000–5005 (2008).
53. González, M. L. *et al.* Mechanism Underlying the Reversal of Drug Resistance in P-Glycoprotein-Expressing Leukemia Cells by Pinorensin and the Study of a Derivative. *Front Pharmacol* **8**, 205 (2017).
54. Laiolo, J. *et al.* Analogues of the Lignan Pinorensin as Novel Lead Compounds for P-glycoprotein (P-gp) Inhibitors. *ACS Med Chem Lett* **9**, 1186–1192 (2018).
55. Galski, H. *et al.* P-glycoprotein-dependent resistance of cancer cells toward the extrinsic TRAIL apoptosis signaling pathway. *Biochem Pharmacol* **86**, 584–596 (2013).
56. Souza, P. S. *et al.* Expression of the multidrug transporter P-glycoprotein is inversely related to that of apoptosis-associated endogenous TRAIL. *Exp Cell Res* **336**, 318–328 (2015).
57. Xie, L. H., Akao, T., Hamasaki, K., Deyama, T. & Hattori, M. Biotransformation of pinorensin diglucoside to mammalian lignans by human intestinal microflora, and isolation of *Enterococcus faecalis* strain PDG-1 responsible for the transformation of (+)-pinorensin to (+)-laricresinol. *Chem Pharm Bull (Tokyo)* **51**, 508–515 (2003).
58. Baek, H. *et al.* The anti-inflammatory role of extranuclear apurinic/aprimidinic endonuclease 1/redox effector factor-1 in reactive astrocytes. *Mol Brain* **9**, 99 (2016).
59. Won, M. *et al.* Novel anti-apoptotic mechanism of A20 through targeting ASK1 to suppress TNF-induced JNK activation. *Cell Death Differ* **17**, 1830–1841 (2010).
60. Ro, H., Soun, K., Kim, E. J. & Rhee, M. Novel vector systems optimized for injecting *in vitro*-synthesized mRNA into zebrafish embryos. *Mol Cells* **17**, 373–376 (2004).

Acknowledgements

This work as supported by the National Research Foundation of Korea (NRF) grant funded by the Korea government (MSIP) (No. 2017R1A2A1A05001225; No. 2017R1A5A2015385; No. 2017R1A2A2A05001340). We thank Prof. Han-Ming Shen (National University of Singapore) for fruitful comments and assistance in the preparation of this article.

Author Contributions

S-R.L. participated in the design of the study, carried out bench experiments and analyzes data. H.S.B., K.K., X.P., E.J. helped carrying out bench experiments related to this study. H.R. helped the experiments for the *in vitro* translation assay. K.Q., I.P., M.N. carried out the experiments for the purification of pinorensin and LC-mass analysis. G.M.H. designed this study and wrote the manuscript with comments from the coauthors, and all authors collaborated on the work.

Additional Information

Supplementary information accompanies this paper at <https://doi.org/10.1038/s41598-019-49909-0>.

Competing Interests: The authors declare no competing interests.

Publisher's note Springer Nature remains neutral with regard to jurisdictional claims in published maps and institutional affiliations.



Open Access This article is licensed under a Creative Commons Attribution 4.0 International License, which permits use, sharing, adaptation, distribution and reproduction in any medium or format, as long as you give appropriate credit to the original author(s) and the source, provide a link to the Creative Commons license, and indicate if changes were made. The images or other third party material in this article are included in the article's Creative Commons license, unless indicated otherwise in a credit line to the material. If material is not included in the article's Creative Commons license and your intended use is not permitted by statutory regulation or exceeds the permitted use, you will need to obtain permission directly from the copyright holder. To view a copy of this license, visit <http://creativecommons.org/licenses/by/4.0/>.

© The Author(s) 2019